01

Carbon-dioxide pressure broadening of water vapor absorption line on the region of $\nu_1 + \nu_2 + \nu_3$ vibrational band

© T.M. Petrova, A.M. Solodov, A.A. Solodov, V.M. Deichuli, A.S. Dudaryonok¶, N.N. Lavrentieva

V.E. Zuev Institute of Atmospheric Optics, Siberian Branch, Russian Academy of Sciences,
634021 Tomsk, Russia

¶e-mail: dudaryon@iao.ru

Received September 05, 2024
Revised October 04, 2024
Accepted October 08, 2024

The water-vapor line profile parameters are necessary to study the planetary atmospheres where the carbon dioxide is the main gas. H_2O absorption lines broadened by the carbon dioxide were recorded using the IFS 125 HR Fourier spectrometer in the range of $8830-9000\,cm^{-1}$. A modified speed-dependent Voigt profile taking into account the dependence of broadening on the relative speed of the colliding molecules was used to approximate the lines. For the first time the parameters of the H_2O absorption lines in the $\nu_1 + \nu_2 + \nu_3$, $2\nu_1 + \nu_2$, $6\nu_2$, $\nu_1 + 3\nu_2$ and $3\nu_2 + \nu_3$ vibrational-rotational bands were determined. The calculations of the broadening coefficients were carried out using a semi-empirical method which uses a correction factor depending on the quantum numbers. The computed room-temperature broadening coefficients of water vapor lines induced by carbon-dioxide pressure are presented; the rotational quantum number of angular momentum J varies from 0 to 9.

Keywords: Water vapor, Martian atmosphere, Venusian atmosphere, line broadening, H_2O-CO_2.

DOI: 10.61011/EOS.2024.10.60051.7044-24

1. Introduction

Owing to a significant variability of temperatures and pressures, the profile parameters of spectral lines of water vapor broadened by the pressure of carbon dioxide are needed to study the evolution and properties of the atmospheres of planets closest to the Earth. Two terrestrial planets of the Solar System (Mars and Venus) have atmospheres dominated by carbon dioxide ($\sim 96\%$), which sets them radically apart from terrestrial conditions. The accuracy of modeling of spectral absorption in carbon dioxide atmospheres is of paramount importance for reconstruction of quantitative characteristics of absorbers (molecule concentrations) and atmospheric conditions (temperature and pressure). The atmosphere of Mars is presently being studied by the Russian ACS spectrometer, which has a resolving power exceeding 50 000, within the $2.2-4.4\,\mu m$ range [1]. Low pressures and temperatures typical of the atmosphere of Mars also correspond to those observed in the upper mesosphere of Venus ($> 70\,km$) located above the planet's opaque cloud layer. The upper mesosphere of Venus is a region where trace gases have been studied in detail by the Venus Express mission only. Further in-depth examination of trace gases is one of the key objectives of future missions to Venus: Shukrayaan-1 [2], which is planned by the Indian Space Agency, and Venera-D [3], which is to be launched by the State Corporation for Space Activities „Roscosmos."

The vertical distribution of water vapor in planetary atmospheres is key to understanding the transport of water and the rate of its loss by planets (i.e., one needs to determine it in order to trace the evolution of water on planets and in their atmospheres).

Compared with broadening by nitrogen and oxygen, the broadening coefficient of water vapor lines induced by carbon dioxide pressure appear to be understudied [4–10]. The results of theoretical and experimental studies of line broadening and shift coefficients within the spectral ranges of $2.7\,\mu m$ ($3060-4370\,cm^{-1}$) and $6\,\mu m$ ($1350-2300\,cm^{-1}$) have been reported in 2019 [5]. Experiments in the $2.7\,\mu m$ spectral region have been performed earlier in [4]. Study [6] was also focused on the analysis of spectra in the $2.7\,\mu m$ region; the absorption spectra of H_2O-CO_2 were recorded again, and the experimental conditions were clarified. Modern profile models were used in calculations, and it was demonstrated that the best model is the Voigt profile, which takes into account the dependence of broadening and shift on the velocities of colliding molecules (quadratic Voigt profile qSDV). A comparison of the broadening coefficients obtained in [6] and the parameters reported by the authors of the present study in [7] reveals their close agreement: the average difference is just 1.3%. We have also expanded the spectral range of research: the broadening and shift coefficients were determined in three spectral regions of $5150-5550$, $6760-7430$, and $10\,100-10\,800\,cm^{-1}$ [8–10]. In the present study, measurement data obtained within the $8830-9000\,cm^{-1}$ range are presented.

The line half-widths calculated using the semi-classical Robert–Bonamy method [12,13], which relies on accurate modeling of the intermolecular potential, takes into account the subtle details of collisions and intramolecular dynamics, and includes a parabolic trajectory approximation, were pre-

sented in [5,11]. We have already calculated the H_2O-CO_2 broadening coefficients using a semi-empirical method [14] supplemented by exact variational wave functions obtained from global variational calculations [15]. Their introduction helps not only refine the calculations of profile parameters, but also extend the domain of applicability of the method to the level of molecular dissociation. The semi-empirical approach used in calculations in [14] featured model parameters that were determined by fitting to the experimental half-width values. In the present study, a semi-empirical method was also applied in calculations.

The paper is organized as follows: Section 2 provides a brief overview of the experimental conditions and the data processing procedure, and key relations of the collisional theory of line broadening and a detailed description of calculations are presented in Section 3. In Section 4, the measured and calculated profile parameters are listed, and the obtained results are also discussed and compared to those reported earlier.

2. Experiment

Absorption spectra of a water molecule broadened by carbon dioxide pressure were measured with a Bruker IFS 125HR Fourier spectrometer (Institute of Atmospheric Optics, Siberian Branch of the Russian Academy of Sciences, Tomsk) within the $8830-9000\,cm^{-1}$ spectral range. A more detailed description of the experimental setup is provided in [16]. The spectrometer was equipped with a tungsten light source, and radiation was detected by an InSb detector cooled with liquid nitrogen. A 24 cm-long cell was mounted in the cell holder of the spectrometer. Absorption spectra of water molecules were recorded at five different CO_2 pressures: 0.092, 0.251, 0.394, 0.541, and 0.693 atm. The pressure of H_2O-CO_2 mixtures was measured using a DVR5 capacitance manometer with a stated uncertainty of 1 mbar. The water vapor pressure varied from 0.092 to 0.0123 mbar and was determined by an MKS Baratron gauge with a state uncertainty of 0.25%. All measurements were performed at room temperature with a spectral resolution of $0.01-0.012\,cm^{-1}$. The resolution was chosen so that it remained smaller than the width of water vapor absorption lines at each buffer gas pressure. The aperture diameter of the interferometer was set to 1.15 mm in accordance with the spectrometer resolution. Apodization was performed using the boxcar function. To enhance the signal-to-noise ratio in absorption spectra measurements, 3000 scans were performed for each buffer gas. The signal-to-noise ratio was determined using the standard OPUS 6.5 software and was found to be 2500 for equal to 1 absorption.

Simultaneous least-squares fitting of spectra recorded under different experimental conditions was performed to determine the parameters of absorption lines of a water molecule. The Voigt profile, which takes into account the dependence of broadening and shift on the velocities of colliding molecules (quadratic Voigt profile qSDV), was used. A fairly simple algorithm for it is provided in [17,18]. The following parameters of spectral lines were determined: position of the center; intensity; self-broadening, broadening, and shift coefficients induced by carbon dioxide pressure; and parameter characterizing the dependence of broadening on the velocity of colliding molecules. Figure 1 shows an example fit of one of the studied absorption lines of a water molecule with two approximating model profiles: the traditional Voigt profile and the qSDV ones. The results of approximation with the Voigt profile are presented for comparison. The bottom panel shows the difference between the experimental and calculated spectra. The water vapor pressure was monitored by the absorption line intensities provided in the HITRAN database [19], and no changes in pressure were noted in the course of experiments.

A detailed analysis of uncertainties in determination of the parameters absorption line recorded using the Fourier spectroscopy method has been performed numerous times (see, e.g., our study [8]). They depend on uncertainties of pressure, temperature, and optical length and errors associated with the process of fitting the spectral line profile. We have demonstrated that statistical errors emerging in parameter fitting are the main sources of uncertainty in coefficients of spectral line broadening. We analyzed isolated absorption lines of water molecules recorded with a high signal-to-noise ratio or lines for which all nearby ones were easily taken into account. This made it possible to reduce the statistical fitting uncertainties significantly and keep the total uncertainty of determination of broadening coefficients for the examined water absorption lines below 1.5–2%.

3. Procedure and details of calculations

The semi-empirical method used for calculations is based on the collisional theory of broadening and modified by the introduction of additional parameters derived from empirical data. The model parameters are determined by fitting the broadening coefficients to experimental values. In our previous studies, we used an approach developed in collaboration with colleagues from University College London. Intramolecular effects were introduced into it on the basis of accurate wave functions and energy levels obtained from variational calculations [20].

This approach incorporates the contributions of all scattering channels induced by molecular collisions; to calculate them, we used the $D^2(ii'|l_1)$ and $D^2(ff'|l_1)$ transition probabilities reconstructed from the Einstein coefficients in the BT2 line list. The scattering channels induced by collisions and allowed by symmetry were taken into account in calculation of the line broadening and shift parameters [15]. A cutoff is needed to select the Einstein coefficients from 500 million values found in the full BT2 list. It was found through data analysis that the contributions of scattering channels with $\omega_{ii'} > 700\,cm^{-1}$

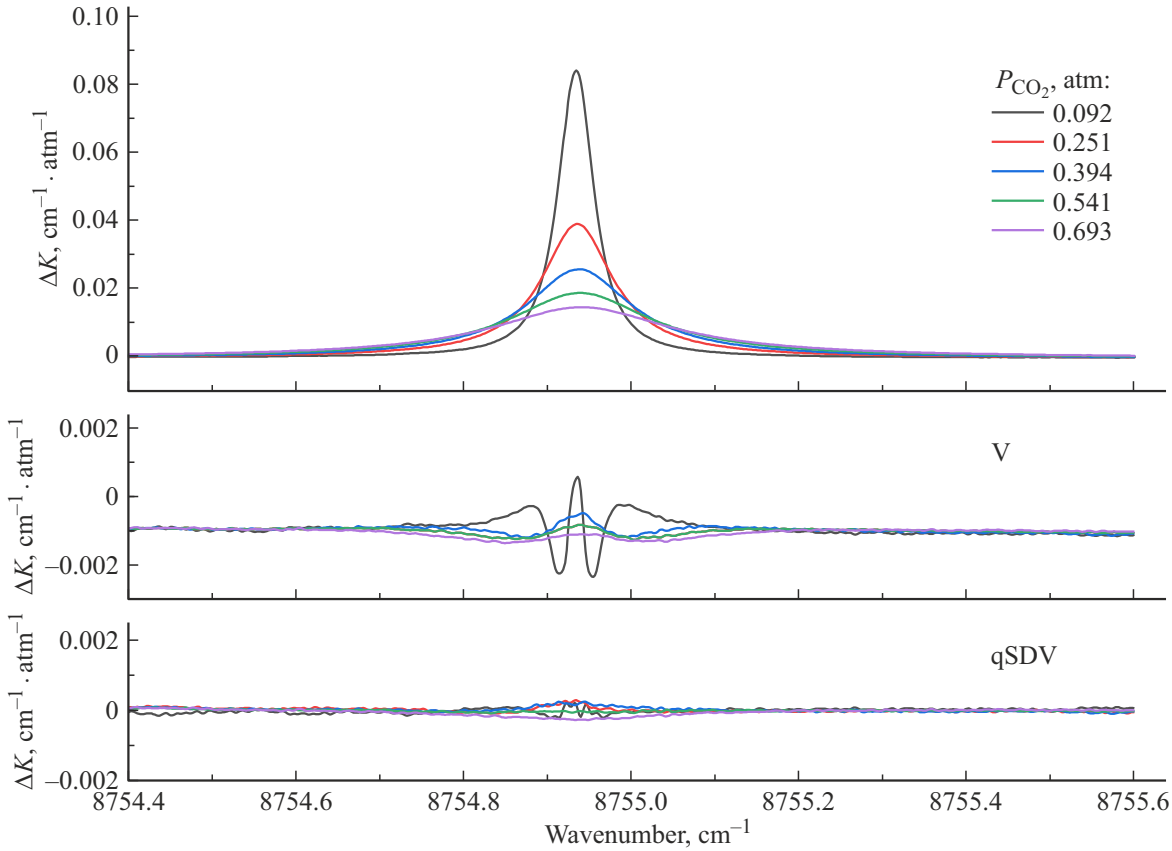


Figure 1. Example experimental spectrum (H_2O absorption line centered at 8751.70991 cm^{-1}) and deviations between the experimental and calculated spectra with fitting by V (middle panel) and qSDV (lower panel) profiles.

and $K_a - K_a' > 3$ may be neglected. It is important to note that the BT2 line list allows one to calculate the water-vapor line profile parameters through to the molecule dissociation limit.

We used the traditional approach with the following expression for half-width:

$$\gamma_{if} = \mathrm{Re}\sum_{\mathrm{int}} \int dvv \int dbb\left(\frac{v}{v'}\right)^2 \times f\left(b, v, l_1, l_2, D^2(ii'|l_1), D^2(ff'|l_1)\right). \quad (1)$$

Integral $\int dv \ldots$ is averaging over collisions; $f(b, \ldots)$ is a certain function containing quantities $D^2(ii'|l_1)$ and $D^2(ff'|l_1)$, which depend on the molecular constants of an absorbing molecule only and are associated with scattering channels $i \to i'$ and $f \to f'$; b is the impact parameter; v is the initial collision velocity; and l_1 and l_2 are the multiplicity indices for the absorbing and perturbing molecules. The integrand in (1) is expanded into a series to obtain [14]

$$\gamma_{\mathrm{if}} = A + \sum D^2(ii'|l)P_{l_1l_2}(\omega_{ii'}) + \sum D^2(ff'|l)P_{l_1l_2}(\omega_{ff'}) + \ldots,$$

$$A = \frac{n}{c}\sum_{j_2}\rho(j_2)\int_0^\infty vdvb_0^2(v, j_2), \quad (2)$$

where $b_0(v, j_2)$ — interruption parameter and $\rho(j_2)$ — population of level j_2 of the perturbing molecule.

The efficiency functions of scattering channels may be written as

$$P_{l_1l_2}(\omega) = P^{\mathrm{ATC}}_{l_1l_2}(\omega)[1+a_1\omega+a_1\omega^2+\ldots] \equiv P^{\mathrm{ATC}}_{l_1l_2}(\omega)C(\omega), \quad (3)$$

where $P^{\mathrm{ATC}}_{l_1l_2}(\omega)$ is the interaction efficiency function in the Anderson–Tsao–Curnutte approximation and the expression in square brackets in equality (3) may be presented in the form of J-dependent expressions the parameters of which are fitted to the experimental half-width values.

The correction factor in (3) was obtained in the following form:

$$C = c_1\left(c_2\sqrt{J}+1\right), \quad (4)$$

where c_1, cc_2 are fitting parameters. The form of the correction factor is determined by analyzing the rotational dependence of half-widths of H_2O–CO_2 lines.

In collisions of H_2O and CO_2 molecules, the primary contribution to the broadening is produced by the interaction between the dipole moment of water vapor (1.8549 D for the ground state) and the quadrupole

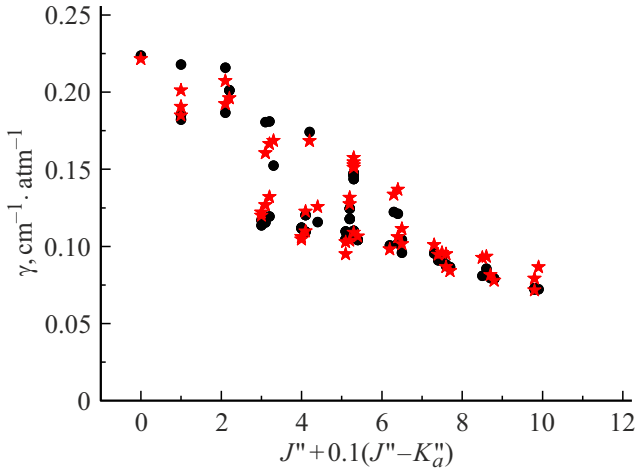


Figure 2. Dependence of experimental (asterisks) and calculated (circles) H_2O-CO_2 absorption line broadening coefficients obtained here on rotational quantum numbers.

moment of carbon dioxide (4.02 DÅ). Induction and dispersion interactions and electrostatic interactions of higher orders, most particularly the quadrupole–quadrupole interactions ($Q_{bb}(H_2O) = -0.13$, $Q_{cc}(H_2O) = -2.50$, $Q_{aa}(H_2O) = 2.63$ DÅ, where a, b and c are the axes of inertia), also play an important role.

4. Discussion

Most transitions in the 8830–9000 cm^{-1} spectral region belong to vibration-rotational band $\nu_1 + \nu_2 + \nu_3$, which is the strongest band within the studied range; several other transitions belong to bands $2\nu_1 + \nu_2$ (five lines), $6\nu_2$ (one line), $\nu_1 + 3\nu_2$ (one line), and $3\nu_2 + \nu_3$ (one line) (Table 1). A total of 50 R-branch lines were analyzed in detail in the present study. Figure 2 presents the measured (qSDV profile) and calculated broadening coefficients of water vapor lines by carbon dioxide pressure as a function of $J'' + 0.5(J'' - K_a'')$. It is evident that the rotational dependences of our experimental and calculated values agree closely. The corresponding root-mean-square deviation (RMSD) is 0.0089 $cm^{-1} \cdot atm^{-1}$ (5.7%). The obtained line half-widths are in close agreement with those calculated by Gamache with the use of the Robert–Bonamy method [11]: the RMSD for calculated data from [11] and our measured (calculated) data is 0.0129 $cm^{-1} \cdot atm^{-1}$ (0.0128 $cm^{-1} \cdot atm^{-1}$).

The experimental line half-widths obtained here and in our previous studies were compared for perpendicular bands ν_3 [7], $\nu_1 + \nu_3$, $2\nu_2 + \nu_3$ [8], $\nu_2 + \nu_3$ [9], $2\nu_1 + \nu_3$, and $\nu_1 + 2\nu_2 + \nu_3$ [10]. Figure 3 reveals identical dependences of the line half-widths on rotational quantum numbers in different absorption bands; notably, the line number corresponds to a broadening coefficient with the same rotational quantum numbers of the upper and lower vibrational states. The RMS values for line half-widths determined here and the experimental data from [7–10] are listed in Table 2.

The existence of a dependence of the broadening coefficients of molecular water absorption lines on vibrational quantum numbers was revealed in our earlier studies (e.g., in [21]) for H_2O–(He, Ar, Kr, and Xe): the broadening coefficients increased with an increase in vibrational excitation. This dependence was manifested clearly in variation of vibrational quantum numbers υ_1 and υ_3, but was very weak when υ_2 was varied. It is not without interest to examine similar dependencies in the case of line broadening by carbon dioxide. We took two sets of absorption lines belonging to bands ν_3, $\nu_2 + \nu_3$, $\nu_1 + \nu_2 + \nu_3$ and $\nu_1 + \nu_3$, $\nu_1 + \nu_2 + \nu_3$, $\nu_1 + 2\nu_2 + \nu_3$. It follows from Fig. 4 that the half-widths of all lines (with the exception of two lines in the $\nu_2 + \nu_3$ band) are smaller than in the $\nu_1 + \nu_2 + \nu_3$

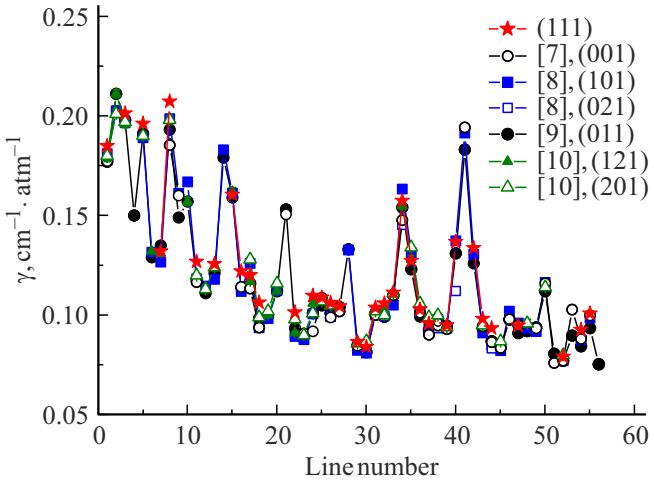


Figure 3. Experimental half-widths (qSDV profile) of H_2O absorption lines obtained in the present study (asterisks) and in [7–10]. Vibrational quantum numbers of the upper state are given in brackets.

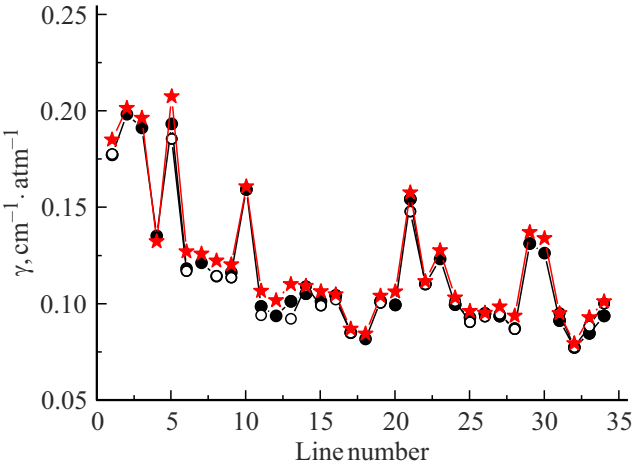


Figure 4. Experimental half-widths of H_2O absorption lines obtained in the present study in the $\nu_1 + \nu_2 + \nu_3$ band (asterisks), in [7] in the ν_3 band (open circles), and in [9] in the $\nu_2 + \nu_3$ band (filled circles).

Table 1. Broadening coefficients of a water lines in the 8830–9000 cm^{-1} region

ν_{HITRAN}, cm^{-1}	$\nu_1\nu_2\nu_3$	$J'K'_aK'_c$	$J''K''_aK''_c$	Experiment		Calculation
				γ, $cm^{-1} \cdot atm^{-1}$	γ^2, $cm^{-1} \cdot atm^{-1}$	γ, $cm^{-1} \cdot atm^{-1}$
8830.230601	1 1 1	1 0 1	0 0 0	0.2215(11)	0.0427(12)	0.2237
8842.895688	2 1 0	4 1 4	3 0 3	0.1685(12)	0.0451(11)	0.1524
8848.069690	1 1 1	2 1 2	1 1 1	0.1849(13)	0.0418(11)	0.1822
8857.463816	2 1 0	2 2 1	1 1 0	0.1906(10)	0.0387(10)	0.1853
8861.124522	1 1 1	2 1 1	1 1 0	0.2012(16)	0.0432(8)	0.2180
8869.871481	1 1 1	3 0 3	2 0 2	0.1961(14)	0.0403(12)	0.2012
8874.582623	2 1 0	3 2 2	2 1 1	0.1923(11)	0.0455(9)	0.1867
8882.871916	1 1 1	4 1 4	3 1 3	0.1320(18)	0.0320(12)	0.1194
8884.497013	1 1 1	3 1 2	2 1 1	0.2072(10)	0.0550(11)	0.2159
8887.786580	2 1 0	4 2 3	3 1 2	0.1665(9)	0.0226(9)	0.1810
8899.130581	1 1 1	4 2 3	3 2 2	0.1268(8)	0.0345(9)	0.1155
8899.692123	1 1 1	5 0 5	4 0 4	0.1257(11)	0.0290(8)	0.1158
8907.902475	1 1 1	4 3 2	3 3 1	0.1221(13)	0.0365(9)	0.1136
8909.111042	1 1 1	4 3 1	3 3 0	0.1201(13)	0.0283(10)	0.1169
8909.361899	1 1 1	4 2 2	3 2 1	0.1605(12)	0.0343(9)	0.1806
8912.255288	1 1 1	6 1 6	5 1 5	0.1064(12)	0.0277(8)	0.1041
8925.221812	1 1 1	7 1 7	6 1 6	0.1015(11)	0.0266(9)	0.0959
8928.477583	1 1 1	5 3 3	4 3 2	0.1098(13)	0.0262(9)	0.1095
8932.529234	1 1 1	5 3 2	4 3 1	0.1226(9)	0.0283(8)	0.1203
8933.461795	1 1 1	5 2 3	4 2 2	0.1683(8)	0.0375(10)	0.1742
8934.739864	1 1 1	6 2 5	5 2 4	0.1089(8)	0.0211(8)	0.1102
8936.261269	1 1 1	5 4 2	4 4 1	0.1062(12)	0.0198(10)	0.1116
8936.408647	1 1 1	5 4 1	4 4 0	0.1045(14)	0.0146(11)	0.1122
8937.130081	1 1 1	8 1 8	7 1 7	0.0867(13)	0.0149(10)	0.0873
8937.233391	1 1 1	8 0 8	7 0 7	0.0842(9)	0.0149(7)	0.0866
8948.149016	1 1 1	9 0 9	8 0 8	0.0778(8)	0.0117(6)	0.0791
8948.441599	1 1 1	9 1 9	8 1 8	0.0815(9)	0.0141(7)	0.0794
8948.763184	1 1 1	6 3 4	5 3 3	0.1039(9)	0.0164(6)	0.1079
8950.333776	1 1 1	7 2 6	6 2 5	0.1060(14)	0.0234(7)	0.1019
8953.478657	1 1 1	6 2 4	5 2 3	0.1574(15)	0.0306(9)	0.1475
8954.129705	0 6 0	6 1 6	5 2 3	0.1545(15)	0.0213(10)	0.1436
8955.053438	1 1 1	7 1 6	6 1 5	0.1114(13)	0.0181(11)	0.1043
8955.722146	1 3 0	6 5 2	5 2 3	0.1526(10)	0.0255(9)	0.1458
8956.293315	1 1 1	6 3 3	5 3 2	0.1274(14)	0.0275(11)	0.1245
8957.196631	1 1 1	6 4 3	5 4 2	0.0951(10)	0.0115(9)	0.1048
8957.600737	1 1 1	10 1 10	9 1 9	0.0716(14)	0.0075(11)	0.0722

Table 1. (*continued*).

8957.866487	1 1 1	6 4 2	5 4 1	0.1029(11)	0.0192(10)	0.1096
8958.633668	1 1 1	10 0 10	9 0 9	0.0866(12)	0.0165(9)	0.0721
8961.842845	0 3 1	6 5 1	5 3 2	0.1317(11)	0.0266(9)	0.1178
8964.611678	1 1 1	8 2 7	7 2 6	0.0959(13)	0.0165(8)	0.0932
8967.232470	1 1 1	8 1 7	7 1 6	0.0950(12)	0.0158(9)	0.0884
8967.743259	2 1 0	6 3 4	5 2 3	0.1510(11)	0.0224(8)	0.1464
8977.364277	1 1 1	7 4 4	6 4 3	0.0982(14)	0.0195(9)	0.1007
8978.857349	1 1 1	9 2 8	8 2 7	0.0935(12)	0.0166(8)	0.0856
8982.124336	1 1 1	7 2 5	6 2 4	0.1368(13)	0.0355(9)	0.1211
8982.757999	1 1 1	7 3 4	6 3 3	0.1337(14)	0.03139(12)	0.1223
8983.703963	1 1 1	8 3 6	7 3 5	0.0948(9)	0.0140(10)	0.0909
8989.799691	1 1 1	10 1 9	9 1 8	0.0792(9)	0.0101(9)	0.0730
8998.963587	1 1 1	9 3 7	8 3 6	0.0927(10)	0.0212(9)	0.0809
9001.653216	1 1 1	8 4 4	7 4 3	0.1009(9)	0.0266(8)	0.0954
9004.172600	1 1 1	8 3 5	7 3 4	0.1358(14)	0.0329(11)	0.1149

Note. ν_1, ν_2, ν_3 — vibrational quantum numbers of the upper level; $J'K'_aK'_c$ and $J''K''_aK''_c$ — rotational quantum numbers of the upper and lower states, respectively; γ — broadening coefficients of H_2O absorption lines induced by the CO_2 pressure; and γ^2 — parameters characterizing the dependence of broadening on the velocity of colliding molecules.

band, with the average difference being 4.6%; the half-widths of absorption lines of the ν_3 and $\nu_2 + \nu_3$ bands match within the experimental error (the difference is 2.2%). Such clear dependences are not observed in the second data set. Although the lines of bands differing only in the bending vibration excitation are considered, there is a difference in the broadening coefficients of H_2O absorption lines with the same set of rotational quantum numbers. It can be seen from Fig. 5 that most of the lines in the $\nu_1 + \nu_2 + \nu_3$ band are, on average, more broadened than those in the $\nu_1 + \nu_3$ and $\nu_1 + 2\nu_2 + \nu_3$ bands (by 4.3 and 2.9%, respectively). These differences may be attributed to the fact that, in keeping with the objective of the Russian Science Foundation grant, the parameters of all strong absorption lines of a water molecule (including those located under one profile) were determined [8].

Table 2. Root-mean-square deviations of our measured/calculated and experimental [8–11] CO_2 pressure broadening coefficients of H_2O lines of the R-branch

Source	Bands	SD, $cm^{-1} \cdot atm^{-1}$
Experiment [7]	ν_3	0.0078
Experiment [8]	$\nu_1 + \nu_3$, $2\nu_2 + \nu_3$	0.0105
Experiment [9]	$\nu_2 + \nu_3$	0.0059
Experiment [10]	$2\nu_1 + \nu_3$, $\nu_1 + 2\nu_2 + \nu_3$	0.0091
Calculation [7]	ν_3	0.0095
Calculation [8]	$\nu_1 + \nu_3$, $2\nu_2 + \nu_3$	0.0109
Calculation [9]	$\nu_2 + \nu_3$	0.0088
Calculation [10]	$2\nu_1 + \nu_3$, $\nu_1 + 2\nu_2 + \nu_3$	0.0114

5. Conclusion

The broadening coefficients for 50 strongest absorption lines of a water molecule belonging to vibration-rotational bands $\nu_1 + \nu_2 + \nu_3$, $2\nu_1 + \nu_2$, $6\nu_2$, $\nu_1 + 3\nu_2$, and $3\nu_2 + \nu_3$ in the $8830-9000\,cm^{-1}$ spectral region were determined. The broadening coefficients obtained using the modified Voigt profile (qSDV) are in good agreement with experimental data [7–11]. The use of modern profile shape models in approximation of molecular H_2O absorption lines broadened by CO_2 pressure made it possible to obtain new highly accurate broadening coefficient values that characterize the spectra at the level of experimental uncertainty. The results of calculations performed using the semi-empirical method agree closely with the measurement data.

The obtained parameters of absorption lines of water broadened by the pressure of carbon dioxide should allow one to determine more accurately the concentration of H_2O in the carbon dioxide atmospheres of planets and calculate these parameters for other spectral regions. Experimental and theoretical studies of the H_2O-CO_2 line shifts and the

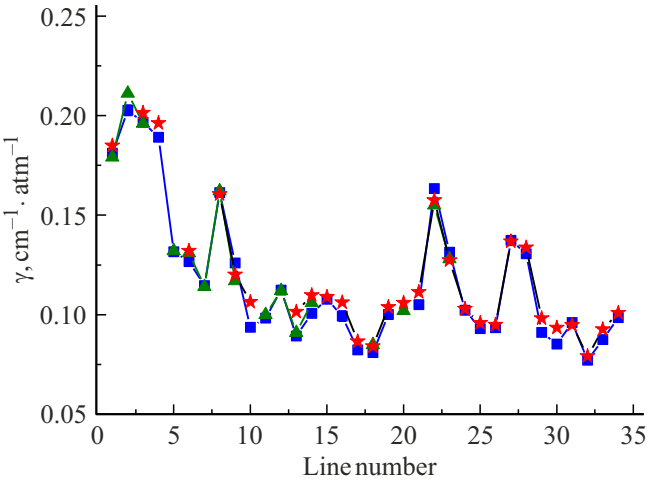


Figure 5. Experimental half-widths of H_2O absorption lines obtained in the present study in the $\nu_1 + \nu_2 + \nu_3$ band (asterisks), in [8] in the $\nu_1 + \nu_3$ band (squares), and in [10] in the $\nu_1 + 2\nu_2 + \nu_3$ band (triangles).

determination of their accurate values within a wide spectral range will be the object of future work.

Funding

This study was carried out as part of project No. 24-22-00170 of the Russian Science Foundation.

Conflict of interest

The authors declare that they have no conflict of interest.

References

[1] O. Korablev, F. Montmessin, A. Trokhimovskiy, A.A. Fedorova, A.V. Shakun, A.V. Grigoriev, B.E. Moshkin, N.I. Ignatiev, F. Forget, F. Lefévre, K. Anufreychik, I. Dzuban, Y.S. Ivanov, Y.K. Kalinnikov, T.O. Kozlova, A. Kungurov, V. Makarov, F. Martynovich, I. Maslov, D. Merzlyakov, P.P. Moiseev, Y. Nikolskiy, A. Patrakeev, D. Patsaev, A. Santos-Skripko, O. Sazonov, N. Semena, A. Semenov, V. Shashkin, A. Sidorov, A.V. Stepanov, I. Stupin, D. Timonin, A.Y. Titov, A. Viktorov, A. Zharkov, F. Altieri, G. Arnold, D.A. Belyaev, J.L. Bertaux, D.S. Betsis, N. Duxbury, T. Encrenaz, T. Fouchet, J.-C. Gérard, D. Grassi, S. Guerlet, P. Hartogh, Y. Kasaba, I. Khatuntsev, V.A. Krasnopolsky, R.O. Kuzmin, E. Lellouch, M.A. Lopez-Valverde, M. Luginin, A. Määttänen, E. Marcq, J. Martin Torres, A.S. Medvedev, E. Millour, K.S. Olsen, M.R. Patel, C. Quantin-Nataf, A.V. Rodin, V.I. Shematovich, I. Thomas, N. Thomas, L. Vazquez, M. Vincendon, V. Wilquet, C.F. Wilson, L.V. Zasova, L.M. Zelenyi, M.P. Zorzano. Space Science Reviews, **214**(1), 1 (2018). DOI: 10.1007/s11214-017-0437-6

[2] N. Shaji. [electronic source]. URL: https://www.lpi.usra.edu/vexag/meetings/archive/vexag17/presentations/Nigar.pdf

[3] D.A. Gorinov, N.A. Eismont, I.D. Kovalenko, A.S. Abbakumov, S.A. Bober. Solar System Research. **53** (7), 506–510 (2019). DOI: 10.1134/S0038094619070244

[4] L.R. Brown, C.M. Humphrey, R.R. Gamache. J. Mol. Spectrosc., **246**, 1 (2007). DOI: 10.1016/j.jms.2007.07.010

[5] R.R. Gamache, S.P. Neshyba, J.J. Plateaux, A. Barbe, L. Regalia, J.B. Pollack. J. Mol. Spectrosc., **170**, 131 (1995). DOI: 10.1006/jmsp.1995.1060

[6] E. Ducreux, B. Grouiez, S. Robert, M. Lepere, B. Vispoel, R.R. Gamache, L. Regalia. J. Quant. Spectrosc. Radiat. Transf., **323**, 109026 (2024). DOI: 10.1016/j.jqsrt.2024.109026

[7] V.M. Deichuli, T.M. Petrova, A.A. Solodov, A.M. Solodov. Atmosp. Ocean. Opt., **35**, 634 (2022).

[8] V.M. Deichuli, T.M. Petrova, A.A. Solodov, A.M. Solodov, A.A. Fedorova. J. Quant. Spectrosc. Radiat. Transf., **293**, 108386 (2022). DOI: 10.1016/j.jqsrt.2023.108850

[9] T.M. Petrova, A.M. Solodov, A.A. Solodov, V.M. Deichuli, N.N. Lavrentieva, A.S. Dudaryonok. J. Quant. Spectrosc. Radiat. Transf., **311**, 108757 (2023). DOI: 10.1016/j.jqsrt.2023.108757

[10] Y.G. Borkov, T.M. Petrova, A.M. Solodov, A.A. Solodov. J. Mol. Spectrosc., **344**, 39 (2018). DOI: 10.1016/j.jms.2017.10.010

[11] L. Régalia, E. Cousin, R.R. Gamache, B. Vispoel, S. Robert, X. Thomas. J. Quant. Spectrosc. Radiat. Transf., **231**, 126 (2019). DOI: 10.1016/j.jqsrt.2019.04.012

[12] D. Robert, J. Bonamy. J. Phys. France, **40**, 923 (1979). DOI: 10.1051/jphys:019790040010092300

[13] Q. Ma, R.H. Tipping, C. Boulet. J. Quant. Spectrosc. Radiat. Transf., **103**, 588 (2007). DOI: 10.1016/j.jqsrt.2006.08.001

[14] A.D. Bykov, N.N. Lavrentieva, L.N. Sinitsa. Mol. Phys., **102**, 1653 (2004). DOI: 10.1080/00268970410001725765

[15] N.N. Lavrentieva, B.A. Voronin, A.A. Fedorova. Opt. Spectr., **118** (1), 11 (2015). DOI: 10.1134/S0030400X15010178.

[16] V.M. Deichuli, T.M. Petrova, A.A. Solodov, A.M. Solodov, V.I. Starikov. Mol. Phys., **121**, 5 (2023). DOI: 10.1080/00268976.2023.2216133

[17] N.H. Ngo, D. Lisak, H. Tran, J.-M. Hartmann. J. Quant. Spectrosc. Radiat. Transf. **129**, 89 (2013). DOI: 10.1016/j.jqsrt.2013.05.034

[18] H. Tran, N.H. Ngo, J.-M. Hartmann. J. Quant. Spectrosc. Radiat. Transf., **129**, 199 (2013). DOI: 10.1016/j.jqsrt.2013.06.015

[19] I.E. Gordon, L.S. Rothman, R.J. Hargreaves, R. Hashemi, E.V. Karlovets, F.M. Skinner, E.K. Conway, C. Hill, R.V. Kochanov, Y. Tan, P. Wcisło, A.A. Finenko, K. Nelson, P.F. Bernath, M. Birk, V. Boudon, A. Campargue, K.V. Chance, A. Coustenis, B.J. Drouin, J.-M. Flaud, R.R. Gamache, J.T. Hodges, D. Jacquemart, E.J. Mlawer, A.V. Nikitin, V.I. Perevalov, M. Rotger, J. Tennyson, G.C. Toon, H. Tran, V.G. Tyuterev, E.M. Adkins, A. Baker, A. Barbe, E. Cané, A.G. Császár, A. Dudaryonok, O. Egorov, A.J. Fleisher, H. Fleurbaey, A. Foltynowicz, T. Furtenbacher, J.J. Harrison, J.-M. Hartmann, V.-M. Horneman, X. Huang, T. Karman, J. Karns, S. Kassi, I. Kleiner, V. Kofman, F. Kwabia-Tchana, N.N. Lavrentieva, T.J. Lee, D.A. Long, A.A. Lukashevskaya, O.M. Lyulin, V.Yu. Makhnev, W. Matt, S.T. Massie, M. Melosso, S.N. Mikhailenko, D. Mondelain, H.S.P. Müller, O.V. Naumenko, A. Perrin, P.L. Polyansky, E. Raddaoui, P.L. Raston, Z.D. Reed, M. Rey, C. Richard, R. Tóbiás, I. Sadiek, D.W. Schwenke,

E. Starikova, K. Sung, F. Tamassia, S.A. Tashkun, J. Vander Auwera, I.A. Vasilenko, A.A. Vigasin, G.L. Villanueva, B. Vispoel, G. Wagner, A. Yachmenev, S.N. Yurchenko. J. Quant. Spectrosc. Radiat. Transf., **277**, 107949 (2022). DOI: 10.1016/j.jqsrt.2021.107949

[20] R.J. Barber, J. Tennyson, G.J. Harris, R.N. Tolchenov. Monthly Notices of the Royal Astronomical Society, **368**, 1087 (2006). DOI: 10.1111/j.1365-2966.2006.10184.x

[21] V.I. Starikov, T.M. Petrova, A.M. Solodov, A.A. Solodov, V.M. Deichuli. Atmos. Oceanic Opt. **36**, 433 (2023). DOI: 10.15372/AOO20230403.

Translated by D.Safin